Molecular Simulation

ISSN: (Print) (Online) Journal homepage: www.tandfonline.com/journals/gmos20

Molecular insights into the corrosion inhibition mechanism of omeprazole and tinidazole: a theoretical investigation

Savaş Kaya, Hassane Lgaz, Abhinay Thakkur, Ashish Kumar, Dilara Özbakır Işın, Nihat Karakuş & Samia Ben Ahmed

To cite this article: Savaş Kaya, Hassane Lgaz, Abhinay Thakkur, Ashish Kumar, Dilara Özbakır Işın, Nihat Karakuş & Samia Ben Ahmed (2023) Molecular insights into the corrosion inhibition mechanism of omeprazole and tinidazole: a theoretical investigation, Molecular Simulation, 49:17, 1632-1646, DOI: 10.1080/08927022.2023.2256888

To link to this article: https://doi.org/10.1080/08927022.2023.2256888

Published online: 25 Sep 2023.

MOLECULAR SIMULATION
2023, VOL. 49, NO. 17, 1632–1646
https://doi.org/10.1080/08927022.2023.2256888

Molecular insights into the corrosion inhibition mechanism of omeprazole and tinidazole: a theoretical investigation

Savaş Kaya[a], Hassane Lgaz [b], Abhinay Thakkur[c], Ashish Kumar[d], Dilara Özbakır Işın[e], Nihat Karakuş[e] and Samia Ben Ahmed[f]

[a]Department of Pharmacy, Sivas Cumhuriyet University, Health Services Vocational School, Sivas, Turkey; [b]Innovative Durable Building and Infrastructure Research Center, Center for Creative Convergence Education, Hanyang University ERICA, Ansan-si, Republic of Korea; [c]Department of Chemistry, School of Chemical Engineering and Physical Sciences, Lovely Professional University, Phagwara, India; [d]NCE, Department of Science and Technology, Bihar Engineering University, Government of Bihar, Phagwara, India; [e]Faculty of Science, Department of Chemistry, Sivas Cumhuriyet University, Sivas, Turkey; [f]Department of Chemistry, College of Sciences, King Khalid University, Abha, Saudi Arabia

ABSTRACT

In many studies published in recent years, corrosion scientists proved that various drug molecules can exhibit high inhibition performance against the corrosion of metal surfaces and alloys. This study presents the adsorption behaviour and inhibition mechanism of Omeprazole and Tinidazole on steel surface in gas phase and aqueous acidic conditions using quantum chemical calculations and molecular dynamics simulations. Well-known quantum chemical parameters such as E_{HOMO}, E_{LUMO}, energy gaps, dipole moment, global hardness, softness, electrophilicity, electrodonating power, electroaccepting power and the fraction of electron transfer, were calculated to understand the corrosion inhibition properties and interactions with the steel surface of the studied molecules. Fukui indices analysis was performed to identify the local reactivities of the molecules. Additionally, Monte Carlo simulations were used to determine the optimal adsorption configuration of the inhibitors onto a Fe (1 1 0) surface. The study's findings provide valuable insights into preventing corrosion of steel surfaces in aqueous acidic environments. The theoretical data obtained was evaluated in terms of Maximum Hardness, Minimum Polarizability and Minimum Electrophilicity Principles.

ARTICLE HISTORY
Received 30 March 2023
Accepted 30 August 2023

KEYWORDS
Corrosion; inhibition; computational analysis; MCS; Fukui indices

1. Introduction

In today's world, preventing metallic corrosion is a crucial issue as metals and alloys are widely used in various industrial applications. Iron and its alloys are particularly important in mechanical industries. In many industrial processes, acid solutions are used for techniques such as acid cleaning, acid pickling and acid descaling. However, these acid solutions can cause serious corrosion on metallic surfaces, leading to significant economic losses for industries. Therefore, preventing corrosion has become a top priority, especially in protecting metallic surfaces from acid-induced corrosion. One effective technique for corrosion inhibition is the use of inhibitors, which are low-cost, efficient and easy to apply. Generally, organic compounds with heteroatoms (N, O, S and P), aromatic rings, π conjugated systems and conjugated aliphatic bonds are considered effective inhibitors [1–3]. Here, we can mention from some published studies as example to the corrosion inhibitor including heteroatoms. Banerjee and coworkers [4] noted that 2-(2-hydroxybenzylideneamino) phenol and its alkyl/acyl substituted compounds are effective corrosion inhibitors for mild steel in corrosive 1 $molL^{-1}$ HCl medium. Same author [5] showed that two newly synthesised diazomethine functionalised long-chain consisting organic molecules, *namely* (3E)-N-((E)-2-(octadecylimino)ethylidene)octadecan-1-amine (ODE) and (3E)-N-((E)-2-(dodecylimino)ethylidene)dodecan-1-amine (DDE) can be used as efficient surface protective lubricant additive. These type inhibitors can adhere to metallic surfaces through physical adsorption (electrostatic interactions) or chemical adsorption (coordination bond) and protect against corrosion. Physical adsorption occurs when charged inhibitor molecules are attracted to charged metallic surfaces, while chemical adsorption involves the formation of coordinate bonds between inhibitor molecules and metals. These adsorption processes create a uniform film on the metallic surface, preventing aggressive acid attacks. However, further research is needed to fully understand the surface phenomenon and factors that determine the strength of interaction. This investigation aims to provide a detailed explanation of the adsorption process and the contributing factors that control it [6–10].

In the past, inhibitive action performance was determined by weight loss measurements, potentiodynamic polarisation and electrochemical impedance spectroscopy [11]. However, these experimental techniques are expensive, time-consuming and sometimes unable to reveal inhibition mechanisms. With advancements in software and hardware related to computational support systems, computer-aided simulation has become a powerful and easy tool for investigating complex corrosion processes and predicting inhibition efficiency well in advance [12,13]. Proper theoretical modelling and

CONTACT Savaş Kaya savaskaya@cumhuriyet.edu.tr

corresponding quantum chemical calculations are particularly efficient in exploring the relationship between the molecular properties of inhibitors and their corrosion inhibition efficiencies. The corrosion inhibition capability of molecules can be determined by various factors, such as the frontier molecular orbital energies, energy gap, dipole moment, global hardness, softness and the fraction of electron transfer from the inhibitors' molecules to the metallic surface. There are several advantages of using computational support systems and computer-aided simulations for investigating complex corrosion processes [14]:

- Cost-effective: Computational simulations are generally more cost effective than traditional experimental techniques.
- Time-efficient: Simulation techniques are often faster than experimental techniques, allowing for more rapid analysis of complex systems.
- Accessibility: Simulation techniques are accessible to researchers regardless of their geographic location or access to expensive laboratory equipment.
- Prediction: Simulation techniques can predict the performance of corrosion inhibitors before they are tested experimentally, reducing the number of experiments needed.
- Mechanism exploration: Simulations can help explore the underlying mechanisms of corrosion and corrosion inhibition, providing a better understanding of the system being studied.
- Molecular properties: Simulations can reveal the relationship between the molecular properties of inhibitors and their corrosion inhibition efficiencies, providing insights into the design of new inhibitors.
- Versatility: Simulations can be applied to a wide range of corrosion systems, making them a versatile tool for corrosion research.

The main goal of the present study is to investigate the corrosion inhibition capabilities of Omeprazole (OMP) and Tinidazole (TND) molecules with the help of quantum chemical calculations and MC simulations. The agreement with previously published experimental research [15] of the theoretical studies will be checked and thanks to chemical reactivity analysis made about for these molecules will shed light on future studies on the design of new inhibitor systems. In the papers recently published, it is seen that many drug molecules also act as an effective corrosion inhibitor. For that reason, we selected OMP and TND chemical systems for theoretically analysis.

2. Computational details

2.1. Quantum chemical assessment

Chemical reactivity analysis is the predicting how atomic or molecular systems will behave under what conditions. In corrosion inhibition researchers, chemical reactivity analysis of the studied inhibitor systems is among the most important parts of the research because effective corrosion inhibitors are the chemical systems with high reactivity. For the chemical reactivity analysis of the studied corrosion inhibitor, DFT computations and Conceptual DFT based reactivity descriptors are widely considered. Density functional theory (DFT) is a widely used computational method for investigating the electronic structure and properties of molecules, materials and surfaces. In recent years, it has been increasingly applied to the field of corrosion inhibition, which is the process of preventing or reducing the corrosion of metals and alloys in various environments. Corrosion inhibition is important for a wide range of industries, including oil and gas, automotive, aerospace and construction. DFT calculations can provide valuable information about the electronic and structural properties of inhibitor molecules and their interactions with metal surfaces. The inhibition efficiency of a molecule can be related to its electronic structure, such as the frontier molecular orbitals, energy gap and charge distribution. DFT calculations can also predict the adsorption energy and geometry of inhibitor molecules on metal surfaces, which are important factors in determining their inhibition efficiency. By using DFT calculations, researchers can screen a large number of inhibitor candidates in a relatively short time, which is a cost-effective and time-saving approach compared to traditional experimental methods. In addition, DFT calculations can provide insights into the mechanisms of corrosion inhibition and help to design new and more effective inhibitors [16].

In this investigation, all calculations were performed using density functional theory (DFT) methods including always the GD3 correction for dispersion [17]. Three optimisations were done using single valance polarisation (SVP) [18], triple-ζ valance polarisation (TZVP) [19] and valance triple-ζ polarisation (def2-TZVP) [20] basis sets having Becke, 3-parameter Lee, Yang and Par (B3LYP) [21], long-range corrected functional Coulomb attenuating Becke, 3-parameter Lee, Yang and Par (CAM-B3LYP) [22,23] and (ωB97XD) [24] range separated hybrid functional including dispersion respectively. The effect of aqueous solvent was taken into account implicitly in the framework of the integral equation formalism (IEF) version of the polarisable continuum model (PCM)[20] with a dielectric constant of $\epsilon = 78.36$ and a refractive index of $n = 1.33$. Geometry optimisations were performed using equilibrium solvation for the respective state (S_0). Frequency calculations were performed for each optimised structure in order to recheck the stability of the geometries both in gas and water. All calculations are done using the Gaussian09 [25] programme suite. Conceptual Density Functional Theory mathematically introduces the chemical potential (μ), electronegativity (χ), hardness (η), softness (σ) as [26]:

$$\mu = -\chi = \left[\frac{\partial E}{\partial N}\right]_{v(r)} \tag{1}$$

$$\eta = \left[\frac{\partial^2 E}{\partial N^2}\right]_{v(r)} \tag{2}$$

$$\sigma = 1/\eta \tag{3}$$

In the given mathematical relations, E and N are the total electronic energy and total number of the electrons of the selected chemical systems, respectively. v(r) given as subscript represents the constant external potential. If one applies the

finite differences approach to the relations presented above, for the calculations of the aforementioned quantum chemical descriptors, we reach to the equations based on ionisation energy and electron affinity of chemical systems.

$$\chi = -\frac{E_{N+1} - E_{N-1}}{2} = \frac{(E_{N-1} - E_N) + (E_N - E_{N+1})}{2} = \frac{I + A}{2} \quad (4)$$

$$\eta = E_{N+1} - 2E_N + E_{N-1} = I - A \quad (5)$$

First (ω_1) and second (ω_2) electrophilicity indices are calculated from the following relations [27,28].

$$\omega_1 = \chi^2/2\eta \quad (6)$$

$$\omega_2 = I.A/I - A \quad (7)$$

For the estimation of the electron transfer amount from inhibitor to metal surface (ΔN) and metal-inhibitor interaction energy (Δψ), the following equations have been derived considering the equalisation processes regarding to the hardness and electronegativity [29,30].

$$\Delta N = \frac{\phi_{Fe} - \chi_{Inh}}{2(\eta_{Fe} + \eta_{inh})} \quad (8)$$

$$\Delta\psi = -\frac{(\phi_{Fe} - \chi_{Inh})^2}{4(\eta_{Fe} + \eta_{inh})} \quad (9)$$

Here, χ_{inh} and η_{inh} denote the electronegativity and hardness of the inhibitor molecules. $\eta_{Fe} = 0$ eV and $\phi_{Fe(110)} = 4.82$ eV were applied to determine the (ΔN) and Δψ, correspondingly. $\phi_{Fe(110)}$ is the work function calculated for Fe (110) surface.

2.2. Fukui indices

Fukui indices are a set of theoretical parameters used in chemistry, especially in the field of organic chemistry, to predict and describe the reactivity of molecules. They are named after Kenichi Fukui, a Japanese chemist who was awarded the Nobel Prize in Chemistry in 1981 for his work on the theory of chemical reactions. Fukui indices are derived from the concept of the frontier molecular orbitals, which are the highest occupied molecular orbital (HOMO) and the lowest unoccupied molecular orbital (LUMO) of a molecule. The HOMO and LUMO are important because they are involved in chemical reactions, and the energy difference between them, known as the HOMO–LUMO gap, is related to the reactivity of the molecule. The Fukui indices are calculated based on the changes in the electron density that occur when a molecule undergoes a small perturbation, such as the addition or removal of an electron. The two main Fukui indices are the nucleophilic Fukui function (f−) and the electrophilic Fukui function (f+), which describe the reactivity of a molecule towards nucleophiles and electrophiles, respectively. The nucleophilic Fukui function describes the propensity of a molecule to donate electrons, while the electrophilic Fukui function describes the propensity of a molecule to accept electrons. These indices are useful for predicting the site of electrophilic or nucleophilic attack in a chemical reaction.

Additionally, Fukui indices were also used to identify the molecules' locations for accepting and donating electrons. Additionally, Fukui functions with Mulliken population evaluation (NPA) was used to determine the local reactivity regions of the compounds under study [31,32].

$$\text{Nucleophilic attack} \rightarrow f_k^+ = P_k(N+1) - P_k(N) \quad (10)$$

$$\text{Electrophilic attack} \rightarrow f_k^- = P_k(N) - P_k(N-1) \quad (11)$$

Herein, $P_k(N)$, $P_k(N-1)$ *and* $P_k(N+1)$ denote the neutral, cationic and anionic Mulliken populations of the molecules.

2.3. Monte Carlo simulations

Monte Carlo (MC) simulations are a computational technique used to model complex systems with a large number of interacting particles. In the field of corrosion inhibition, MC simulations are employed to study the interaction between inhibitor molecules and metal surfaces. In MC simulations, the behaviour of a system is modelled using random numbers and probabilities. The simulation starts with a random configuration of the system, and then successive random changes are made to the system. At each step, the probability of accepting the change is calculated based on the energy of the system before and after the change. By repeating these steps many times, the simulation samples the configuration space of the system, and statistical properties can be calculated [33,34].

In the context of corrosion inhibition, MC simulations can be used to study the adsorption of inhibitor molecules on metal surfaces. The simulation can calculate the free energy change of the adsorption process, which is related to the inhibition efficiency of the molecule. The simulation can also provide information about the orientation and conformation of the inhibitor molecules on the surface, as well as the distribution of the molecules in the solvent. MC simulations are a useful tool for predicting the corrosion inhibition efficiency of new inhibitor molecules, without the need for costly and time-consuming experimental studies. The simulations can be used to screen large libraries of potential inhibitors, and identify promising candidates for further study.

In this particular study, the Monte Carlo simulation method was employed to investigate the synergistic effect of two compounds on the adsorption behaviour onto the surface of mild steel. The simulation was carried out using the Materials Studio 2017 software, which includes an adsorption locator module. The simulation system was optimised using the COMPASS [35] forcefield, and a Fe (1 1 0) surface was constructed with a 30 Å edge and enlarged to create a supercell (12×12). The inhibitors were then introduced into the simulation system in the presence of 186 water molecules, $4H_3O^+$ ions, and $4Cl^-$ ions. The adsorption energies of the inhibitors onto the surface of iron were calculated and analysed to identify the most stable adsorbed configuration of the studied molecules on the surface of the iron. The higher negative adsorption energy values indicated the most stable configuration of the inhibitors on the iron surface.

2.4. In silico approaches for environmental toxicity and solubility analysis

In silico approaches can be used to predict the environmental toxicity and solubility of corrosion inhibitors. These approaches involve the use of chemical databases and modelling environments to simulate the behaviour of the inhibitors in the environment and predict their potential impact on the ecosystem. One such tool is the Chemical Database with Modelling Environment (CDME) website, which provides a platform for predicting the properties of chemicals including corrosion inhibitors. The website provides access to a range of predictive models that can be used to estimate the physicochemical and toxicological properties of chemicals, including solubility and environmental toxicity. For example, the CDME website can be used to predict the solubility of corrosion inhibitors in water or other solvents based on their molecular structure. The website uses predictive models based on quantitative structure–property relationships (QSPRs) to estimate solubility based on a range of molecular descriptors such as molecular weight, polar surface area, and hydrogen bond donors and acceptors. Similarly, the CDME website can be used to predict the environmental toxicity of corrosion inhibitors based on their chemical structure. The website provides access to a range of predictive models that can estimate the toxicity of chemicals to different organisms, including fish, algae and bacteria. These models use a range of molecular descriptors and toxicological endpoints to predict the potential impact of chemicals on the environment.

3. Results and discussion

3.1. Comparative experimental studies between two studied inhibitors

Al-Nami et al. [15] recently conducted wet chemical experiments to investigate the corrosion inhibition effect of Helicure drugs (OMP and TND) on mild steel surfaces in 1M HCl solution. In the experimental studies, authors used weight loss and Potentiodynamic polarisation (PP) methods because they are widely preferred in experimental corrosion inhibition studies. Table 1 shows the molecular structures, names and abbreviations of OMP and TND (Helicure drugs). The results showed that the inhibitors were highly effective in inhibiting corrosion, with a maximum protection efficiency of 85.8% observed in the presence of 300 ppm OMP + TND during polarisation. The AFM roughness data indicated that the adsorption of OMP + TND on the mild steel surface led to the formation of a protective layer, resulting in a smoother surface and inhibition of corrosive ion attack. However, the authors were unable to fully explain the relative inhibition order of the two inhibitors, which was based on the presence of heteroatoms and aromatic rings. To better understand the inhibition mechanism and explain the trend in inhibition efficiency, the present study employed quantum chemical calculations and Monte Carlo simulations. The study also included a correlation analysis between observed molecular parameters and experimentally obtained inhibition efficiency outcomes.

3.1.1. DFT

In corrosion inhibition, DFT calculations are used to study the adsorption of inhibitor molecules onto the metal surface. The adsorption energy of the inhibitor molecule onto the metal surface is a key factor in determining its effectiveness as a corrosion inhibitor. The higher the adsorption energy, the stronger the bond between the inhibitor and the metal surface, and the better the protection against corrosion. DFT calculations can also provide information on the electronic properties of the inhibitor molecules, such as the distribution of electron density and the electronic structure of the inhibitor-metal interface. This information can be used to understand the mechanism of inhibition and to design more effective inhibitors. Herein, DFT methods were utilised in the calculations, with the GD3 correction for dispersion always included. Optimisation was done using three basis sets: single valance polarisation (SVP), triple-ζ valance polarisation (TZVP) and valance triple-ζ polarisation (def2-TZVP), with the B3LYP, CAM-B3LYP and ωB97XD functionals, respectively. The aqueous solvent effect was considered implicitly using the integral equation formalism (IEF) version of the polarisable continuum model (PCM) with a dielectric constant of $\epsilon = 78.36$ and a refractive index of n = 1.33. Geometry optimisations were performed using equilibrium solvation for the respective state (S_0), and frequency calculations were performed to verify the stability of the geometries both in gas and in water. All calculations were performed using the Gaussian09 programme suite.

The Figure 1 provided shows the calculation results for the adsorption energies of two inhibitors, OMP and TIN, using three different Density Functional Theory (DFT) methods: B3LYP with single valence polarisation (SVP) basis set, CAM-B3LYP with triple-ζ valence polarisation (TZVP) basis set, and wB97XD with valence triple-ζ polarisation (def2-TZVP) basis set in the gas phase. While DFT calculations are often used to study molecules in solution, it is also important to consider the gas-phase geometry of molecules. This is because the gas-phase geometry represents the idealised structure of a molecule, in the absence of solvent effects or intermolecular interactions. Studying DFT-optimised structures in the gas phase allows researchers to gain insights into the intrinsic properties of chemical compounds, without the confounding effects of solvent or intermolecular interactions. For example, gas-phase geometry optimisations can provide information about the stability and reactivity of molecules, as well as the nature of the electronic transitions that occur in chemical reactions.

In addition, gas-phase geometry optimisations are important for benchmarking different computational methods and for comparing theoretical predictions with experimental results. By comparing the gas-phase geometries of molecules with experimental data, researchers can assess the accuracy of their computational methods and make improvements to their models.

Table 2 provides energetic parameters and quantum chemical descriptors for the Omeprazole (OMP) compound, calculated using different DFT methods in both gas and solvent (water) phases. The physio-chemical properties studied include optimisation energy, polarisability, dipole moment,

Table 1. Molecular structures, names and abbreviations of studied inhibitors (Helicure drug).

Abbreviation	Structures	Nomenclature (IUPAC)
TID	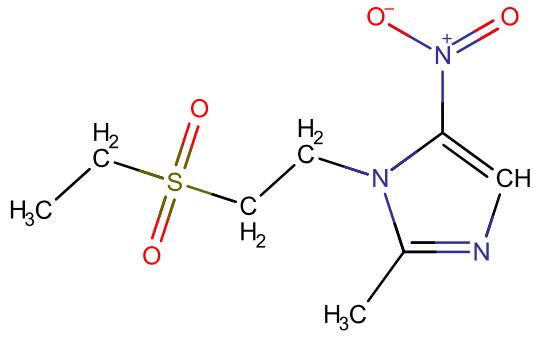	1-[2-(ethanesulfonyl)ethyl]-2-methyl-5-nitro-1H-imidazole ***Tinidazole***
OMP	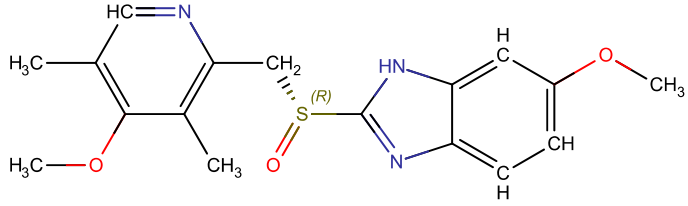	6-methoxy-2-[(R)-(4-methoxy-3,5-dimethylpyridin-2-yl)methanesulfinyl]-1H-1,3-benzodiazole ***Omeprazole***

HOMO (highest occupied molecular orbital), LUMO (lowest unoccupied molecular orbital), ionisation potential (I), electron affinity (A), chemical hardness (η), chemical softness (ζ), electro-negativity (χ), chemical potential (μ) and electrophilicity index (ω). The results show that the energetic parameters and quantum chemical descriptors are different for different DFT methods and between the gas and solvent phases. In general, the CAM-B3LYP/TZVP method produces the most stable optimisation energy for both the gas and solvent phases, while the ωB97XD/Def2-TZVP method produces the least stable optimisation energy. The quantum chemical descriptors include the HOMO (Highest Occupied Molecular Orbital) and LUMO (Lowest Unoccupied Molecular Orbital) energies (in eV), which are important in understanding the reactivity and stability of the molecule. The HOMO–LUMO gap (ΔeV) is the energy difference between the HOMO and LUMO levels. The Ionisation Potential (I) (in eV) is the energy required to remove an electron from the molecule, while the Electron Affinity (A) (in eV) is the energy released when an electron is added to the molecule. The Chemical Hardness (η) (in eV) is a measure of the resistance of the molecule to changes in electron density. The Chemical Softness (σ) (in

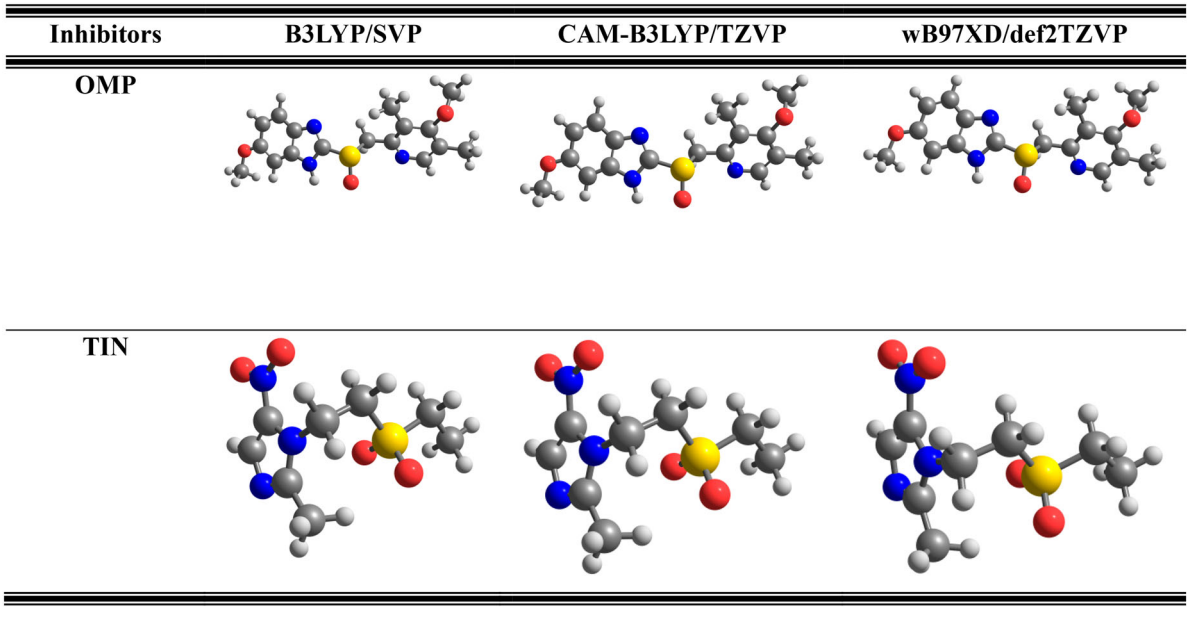

Figure 1. (Colour online) Optimised structures of the studied inhibitor molecules in the gas phase.

Table 2. Energetic Parameters and quantum chemical descriptors for Omeprazole compound by using different DFT methods in both gas and in solvent (water).

OMP	B3LYP/SVP		CAM-B3LYP/TZVP		ωB97XD/Def2-TZVP	
Property	gas	water	gas	water	gas	water
Optimisation energy (a.u.)	−1446.475	−1446.493	−1447.183	−1447.205	−1447.389	−1447.409
Polarisability (a.u.)	250.380	322.519	254.091	333.069	260.892	345.372
Dipole Moment (Debye)	1.846	2.593	2.390	3.378	1.949	3.431
HUMO (eV)	−5.779	−5.934	−7.321	−7.471	−7.757	−7.929
LUMO (eV)	−1.111	−1.285	−0.052	−0.071	−0.733	−0.496
HOMO–LUMO Gap	4.668	4.649	7.269	7.4	7.024	7.433
Ionisation Potential (I)	5.779	5.934	7.321	7.471	7.757	7.929
Electron Affinity (A)	1.111	1.285	0.052	0.071	0.733	0.496
Chemical Hardness (η)	4.668	4.649	7.269	7.4	7.024	7.433
Softness (σ)	0.214	0.215	0.138	0.135	0.142	0.135
Electronegativity (χ)	3.445	3.6095	3.6865	3.771	4.245	4.2125
Chemical Potential (μ)	−3.445	−3.6095	−3.6865	−3.771	−4.245	−4.2125
First Electrophilicity Index (ω_1)	1.271	1.401	0.935	0.961	1.283	1.194
Second Electrophilicity Index (ω_2)	1.375	1.640	0.052	0.072	0.809	0.529
ΔN	0.147	0.130	0.078	0.071	0.041	0.041
Δψ	−0.101	−0.079	−0.044	−0.037	−0.012	−0.012

eV) is the reciprocal of the Chemical Hardness and indicates the ease with which the molecule can be polarised. Electronegativity (χ) (in eV) is a measure of the ability of an atom to attract electrons to itself in a chemical bond. The Chemical Potential (μ) (in eV) is the derivative of the energy with respect to the number of electrons in the molecule. Finally, the Electrophilicity Index (ω) is a measure of the reactivity of the molecule towards electron-rich species. Table 2 analysed that the polarisability and dipole moment increase in the solvent phase compared to the gas phase, indicating an increase in the molecule's ability to interact with other molecules in the solvent. The HOMO–LUMO energy gap decreases in the solvent phase, suggesting that the molecule's reactivity increases in the solvent. The ionisation potential (I) and electron affinity (A) show opposite trends between the gas and solvent phases, indicating that the OMP molecule is more likely to gain an electron in the gas phase, while it is more likely to lose an electron in the solvent phase. The chemical hardness (η) and softness (ζ) show that OMP is a relatively hard molecule, meaning that it is less likely to undergo chemical reactions, and it requires more energy to excite an electron from the HOMO to the LUMO. The electro-negativity (χ) and chemical potential (μ) indicate that OMP has a relatively high electron-attracting ability and a low electron-donating ability. Finally, the electrophilicity index (ω) shows that OMP is a moderate electrophile, meaning that it can accept electrons from nucleophiles to form new chemical bonds.

Table 3 presents the energetic parameters and quantum chemical descriptors for the Tinidazole compound calculated using three different Density Functional Theory (DFT) methods, namely B3LYP/SVP, CAM-B3LYP/TZVP and ωB97XD/Def2-TZVP, in both gas and water solvent phases. The following discussion elaborates on the findings presented in the table. The optimisation energy of the Tinidazole molecule is the lowest in the gas phase, as indicated by the negative values of the optimisation energy in all three DFT methods. However, the presence of the water solvent leads to a slight increase in the optimisation energy, indicating that the molecule is less stable in the solvent phase than in the gas phase. The polarisability of the molecule is higher in the solvent phase than in the gas phase for all DFT methods, indicating that the presence of water enhances the ability of the molecule to polarise. Similarly, the dipole moment of the molecule increases in the presence of water, indicating that the molecule is more polar in the solvent phase.

The HOMO–LUMO energy gap (ΔE) is an important descriptor of the molecule's reactivity. A smaller ΔE value indicates that the molecule is more susceptible to undergo chemical reactions. In the present case, all DFT methods predict a smaller ΔE value in the solvent phase than in the gas phase, suggesting that the molecule is more reactive in water than in the gas phase. The ionisation potential (I) and electron affinity (A) of the molecule indicate its ability to donate and accept electrons, respectively. All three DFT methods predict that the ionisation potential is higher in the solvent phase than in the gas phase, indicating that the molecule is less likely to donate electrons in the presence of water. On the other hand, the electron affinity is higher in the solvent phase than in the gas phase, indicating that the molecule is more likely to accept electrons in the presence of water. The chemical hardness (η) and softness (ζ) of the molecule provide information about its stability and reactivity, respectively. The η value is lower in the solvent phase than in the gas phase, indicating that the molecule is less stable in the presence of water. The ζ value is higher in the solvent phase than in the gas phase, indicating that the molecule is more reactive in water. The electronegativity (χ) and chemical potential (μ) of the molecule indicate its ability to attract and donate electrons, respectively. The χ and μ values are higher in the solvent phase than in the gas phase, indicating that the molecule has a higher affinity for electrons and is more likely to donate electrons in the presence of water. Finally, the electrophilicity index (ω) of the molecule provides information about its ability to act as an electrophile in a chemical reaction. All three DFT methods predict a higher ω value in the solvent phase than in the gas phase, indicating that the molecule is more likely to act as an electrophile in water than in the gas phase. In summary, the presence of water affects the physiochemical properties of the Tinidazole molecule, making it less stable and more reactive. The results also show that the choice of the DFT method affects the values of the calculated parameters, highlighting the importance of selecting an appropriate method for accurate predictions.

Table 3. Energetic Parameters and quantum chemical descriptors for Tinidazole compound by using different DFT methods in both gas and in solvent (water).

TND	B3LYP/SVP		CAM-B3LYP/TZVP		ωB97XD/Def2-TZVP	
Property	gas	water	gas	water	gas	water
Optimisation energy (a.u.)	−1175.209	−1175.228	−1175.830	−1175.853	−1175.990	−1176.010
Polarisability (a.u.)	134.976	176.932	143.261	191.808	145.004	194.998
Dipole Moment (Debye)	5.220	7.066	5.497	7.702	5.045	7.172
HUMO (eV)	−6.951	−7.07	−8.591	−8.713	−9.057	−9.172
LUMO (eV)	−2.432	−2.638	−0.413	−1.641	−0.62	−0.848
HOMO–LUMO Gap	4.519	4.432	8.178	7.072	8.437	8.324
Ionisation Potential (I)	6.951	7.07	8.591	8.713	9.057	9.172
Electron Affinity (A)	2.432	2.638	0.413	1.641	0.62	0.848
Chemical Hardness(η)	4.519	4.432	8.178	7.072	8.437	8.324
Softness (σ)	0.221	0.226	0.122	0.141	0.119	0.120
Electronegativity (χ)	4.6915	4.854	4.502	5.177	4.8385	5.01
Chemical Potential (μ)	−4.6915	−4.854	−4.502	−5.177	−4.8385	−5.01
First Electrophilicity Index (ω_1)	2.435	2.658	1.239	1.895	1.387	1.508
Second Electrophilicity Index (ω_2)	3.741	4.208	0.434	2.022	0.666	0.934
ΔN	0.014	−0.004	0.019	−0.025	−0.001	−0.011
Δψ	−0.001	0.000	−0.003	−0.005	0.000	−0.001

3.2. Fukui indices

Fukui indices are used to study the reactivity of molecules towards different electrophilic and nucleophilic attacks [36–40]. In the context of corrosion inhibition, Fukui indices can provide insight into the inhibitory mechanism of a compound. For example, if a molecule has a high positive Fukui index value at the site of a reactive group, it indicates a high potential for nucleophilic attack at that site. In the case of corrosion inhibition, this could mean that the molecule is able to interact with the metal surface through electrostatic interactions, forming a protective layer and inhibiting further corrosion. On the other hand, if a molecule has a high negative Fukui index value at the site of a reactive group, it indicates a high potential for the electrophilic attack at that site. In the context of corrosion inhibition, this could mean that the molecule is able to donate electrons to the metal surface, thereby reducing the rate of oxidation and corrosion. Additionally, Fukui indices were also used to identify the molecules' locations for accepting and donating electrons. Additionally, Fukui functions with Mulliken population evaluation (NPA) were used to determine the local reactivity regions of the compounds under study using equations (10) and (11).

The Table 4 shows the order of reactive sites of the Omeprazole compound using different DFT/B3LYP/SVP methods in gas and solvent (water). The Fukui indices were calculated for each reactive site, and they were classified into three categories: f^+, f^- and f^0. The Fukui index measures the sensitivity of a molecule's electronic structure to changes in its electronic state. It can help predict which sites in a molecule are most likely to react with other molecules or undergo chemical transformations. In the case of corrosion inhibition, knowing the order of reactive sites can help identify which sites are most likely to react with corrosive agents and which sites are most effective in inhibiting the corrosion process. In the table, the Omeprazole compound has 40 reactive sites, which are labelled from 1S to 40H. The Fukui indices were calculated using the B3LYP/SVP method in gas and water solvent. The results show that the order of reactive sites varies depending on the method and solvent used. For example, in the gas phase, site 17C has the highest f^+value of 0.053, followed by site 34H with a value of 0.056. In water, site 17C still has the highest f^+value, but it increased to 0.097. Site 39H has the second-highest f^+ value in water with a value of 0.049. On the other hand, site 8C has the lowest f^- value in gas and water, indicating that

Table 4. Order of reactive sites (Fukui indices) of compound Omeprazole by using different DFT/B3LYP/SVP methods in both gas and in solvent (water).

Inhibitor	B3LYP/SVP			B3LYP/SVP		
-OMP	*Gas*			*Water*		
	f^+	f^-	f^0	f^+	f^-	f^0
1S	0.055	0.044	0.049	0.046	0.062	0.054
2O	0.008	0.009	0.008	0.002	0.007	0.004
3O	0.082	0.045	0.063	0.052	0.043	0.047
4O	0.062	0.015	0.039	0.082	0.011	0.047
5N	0.003	0.005	0.004	0.008	0.010	0.009
6N	0.033	0.034	0.034	0.036	0.046	0.041
7N	0.006	0.023	0.014	0.006	0.028	0.017
8C	−0.010	0.009	−0.001	−0.008	0.012	0.002
9C	0.010	0.033	0.021	0.004	0.045	0.024
10C	0.007	0.005	0.006	0.008	0.020	0.014
11C	0.039	0.037	0.038	0.068	0.058	0.063
12C	0.020	0.004	0.012	0.030	0.010	0.020
13C	0.017	0.032	0.025	0.005	0.031	0.018
14C	0.023	−0.007	0.008	0.053	0.001	0.027
15C	0.007	0.028	0.017	0.005	0.037	0.021
16C	−0.007	−0.011	−0.009	−0.002	−0.006	−0.004
17C	0.053	0.045	0.049	0.097	0.051	0.074
18C	0.024	0.026	0.025	0.010	0.036	0.023
19C	0.035	0.051	0.043	0.058	0.061	0.060
20C	0.017	0.019	0.018	0.035	0.016	0.026
21C	0.035	0.018	0.027	0.060	0.025	0.042
22C	−0.005	−0.010	−0.008	0.000	−0.003	−0.001
23C	−0.014	−0.024	−0.019	−0.002	−0.009	−0.005
24C	−0.037	−0.021	−0.029	−0.028	−0.008	−0.018
25H	0.030	0.034	0.032	0.024	0.043	0.033
26H	0.030	0.037	0.034	0.025	0.044	0.034
27H	0.026	0.024	0.025	0.026	0.022	0.024
28H	−0.004	0.013	0.005	0.005	0.018	0.011
29H	0.027	0.034	0.031	0.006	0.018	0.012
30H	0.018	0.029	0.024	0.007	0.025	0.016
31H	0.047	0.039	0.043	0.049	0.025	0.037
32H	0.032	0.050	0.041	0.007	0.032	0.020
33H	0.051	0.045	0.048	0.046	0.033	0.040
34H	0.056	0.048	0.052	0.052	0.028	0.040
35H	0.020	0.033	0.027	0.004	0.018	0.011
36H	0.026	0.041	0.033	0.005	0.025	0.015
37H	0.022	0.035	0.028	0.004	0.023	0.014
38H	0.022	0.034	0.028	0.002	0.011	0.007
39H	0.005	0.014	0.010	0.002	0.010	0.006
40H	0.012	0.018	0.015	0.002	0.010	0.006
41H	0.036	0.016	0.026	0.040	0.010	0.025
42H	0.044	0.030	0.037	0.030	0.009	0.019
43H	0.037	0.017	0.027	0.040	0.010	0.025

it is the least likely to react with other molecules. The results also show that the f^- values of the different sites are generally low, which suggests that Omeprazole is not likely to undergo nucleophilic attacks.

Table 5 shows the order of reactive sites, as determined by the Fukui indices, for the compound Omeprazole using different DFT/CAM-B3LYP/TZVP methods in both gas and water solvent. The compound Omeprazole consists of 40 atoms, including carbon, hydrogen, oxygen, nitrogen and sulphur. The table lists the different atoms in Omeprazole, labelled 1S through 40H, and the calculated values of the Fukui indices for each atom using two different DFT/CAM-B3LYP/TZVP methods, one in the gas phase and the other in a water solvent. The Fukui indices indicate the relative susceptibility of each atom to nucleophilic or electrophilic attack. A positive value indicates that the atom is more susceptible to electrophilic attack, whereas a negative value indicates that the atom is more susceptible to nucleophilic attack. A value of zero means that the atom is neither more susceptible to nucleophilic nor electrophilic attack. The table shows that the order of reactive sites varies depending on the method used and whether the calculation is done in gas or water solvent. For example, for the gas phase calculation, the most reactive site is the 17C atom, while in a water solvent, it is the 21C atom. Similarly, the least reactive site in the gas phase is 16C, while in a water solvent, it is 24C.

Table 6 shows the order of reactive sites (Fukui indices) of Omeprazole inhibitor using different DFT/ωB97XD/def2-TZVP methods in both gas and solvent (water) phases. In gas phase, the order of reactive sites for Omeprazole is 4O > 17C > 39H > 33H > 34H > 1S > 3O > 11C > 14C > 21C > 19C > 6N > 25H > 26H > 31H > 2O > 13C > 20C > 29H > 7N > 15C > 10C > 5N > 30H > 38H > 37H > 36H > 35H > 22C > 9C > 12C > 16C > 18C > 28H > 8C > 23C > 27H > 24C. This means that the most reactive sites are the oxygen atom at position 4 (4O), followed by the carbon atom at position 17 (17C), and hydrogen atoms at positions 39 (39H), 33 (33H) and 34 (34H). In the water phase, the order of reactive sites for

Table 5. Order of reactive sites (Fukui indices) of compound Omeprazole by using different DFT/CAM-B3LYP/TZVP methods in both gas and in solvent (water).

Inhibitor -OMP	CAM-B3LYP/TZVP			CAM-B3LYP/TZVP		
	Gas			*Water*		
	f^+	f^-	f^0	f^+	f^-	f^0
1S	0.047	0.063	0.055	0.028	0.107	0.067
2O	0.006	0.014	0.010	0.001	0.008	0.004
3O	0.055	0.053	0.054	0.029	0.051	0.040
4O	0.086	0.015	0.051	0.105	0.010	0.057
5N	0.020	0.003	0.011	0.032	0.015	0.024
6N	0.033	0.016	0.025	0.032	0.040	0.036
7N	−0.004	0.025	0.010	0.003	0.032	0.017
8C	−0.022	0.025	0.001	−0.010	0.033	0.012
9C	0.002	0.036	0.019	0.001	0.035	0.018
10C	0.006	0.002	0.004	0.004	0.032	0.018
11C	0.043	0.038	0.040	0.056	0.073	0.065
12C	0.006	0.005	0.006	0.004	0.006	0.005
13C	0.010	0.037	0.024	0.001	0.020	0.010
14C	0.062	−0.012	0.025	0.102	0.000	0.051
15C	−0.006	0.021	0.008	0.002	0.044	0.023
16C	−0.009	−0.009	−0.009	0.001	−0.001	0.000
17C	0.080	0.043	0.061	0.125	0.046	0.085
18C	0.011	0.028	0.020	0.003	0.030	0.017
19C	0.044	0.061	0.052	0.057	0.070	0.064
20C	0.044	0.016	0.030	0.074	0.021	0.048
21C	0.037	0.003	0.020	0.069	0.017	0.043
22C	0.006	0.005	0.006	0.001	0.006	0.004
23C	−0.008	−0.024	−0.016	0.000	−0.004	−0.002
24C	−0.027	−0.012	−0.020	−0.015	−0.003	−0.009
25H	0.019	0.030	0.025	0.016	0.039	0.028
26H	0.023	0.039	0.031	0.015	0.039	0.027
27H	0.032	0.023	0.028	0.023	0.021	0.022
28H	−0.015	0.010	−0.003	0.002	0.013	0.007
29H	0.021	0.032	0.026	0.003	0.013	0.008
30H	0.010	0.035	0.023	0.003	0.023	0.013
31H	0.056	0.033	0.045	0.040	0.015	0.027
32H	0.020	0.052	0.036	0.002	0.021	0.012
33H	0.064	0.041	0.053	0.041	0.024	0.032
34H	0.067	0.044	0.056	0.050	0.019	0.034
35H	0.010	0.028	0.019	0.001	0.011	0.006
36H	0.014	0.037	0.025	0.001	0.016	0.009
37H	0.012	0.033	0.022	0.001	0.018	0.010
38H	0.015	0.035	0.025	0.001	0.008	0.004
39H	−0.001	0.013	0.006	0.001	0.007	0.004
40H	0.009	0.017	0.013	0.001	0.007	0.004
41H	0.038	0.011	0.025	0.036	0.006	0.021
42H	0.043	0.024	0.034	0.024	0.005	0.015
43H	0.039	0.012	0.026	0.036	0.006	0.021

Table 6. Order of reactive sites (Fukui indices) of compound Omeprazole by using different DFT/ωB97XD/def2-TZVP methods in both gas and in solvent (water).

Inhibitor -OMP	ωB97XD/def2-TZVP			ωB97XD/def2-TZVP		
	Gas			*Water*		
	f^+	f^-	f^0	f^+	f^-	f^0
1S	0.048	0.070	0.059	0.027	0.087	0.057
2O	0.007	0.012	0.009	0.001	0.003	0.002
3O	0.053	0.054	0.054	0.030	0.045	0.037
4O	0.096	0.021	0.059	0.115	0.020	0.068
5N	0.026	0.012	0.019	0.036	0.035	0.035
6N	0.038	0.027	0.033	0.035	0.054	0.045
7N	−0.007	0.015	0.004	0.002	0.006	0.004
8C	−0.012	0.006	−0.003	−0.006	−0.006	−0.006
9C	−0.008	0.029	0.011	−0.003	−0.002	−0.003
10C	0.003	0.011	0.007	0.003	0.014	0.008
11C	0.052	0.063	0.057	0.063	0.133	0.098
12C	0.016	−0.007	0.005	0.019	−0.014	0.003
13C	0.007	0.020	0.013	0.001	0.002	0.001
14C	0.066	−0.004	0.031	0.108	0.008	0.058
15C	−0.005	0.015	0.005	0.003	0.011	0.007
16C	−0.008	−0.015	−0.012	−0.001	−0.006	−0.003
17C	0.075	0.060	0.067	0.114	0.115	0.115
18C	0.011	0.029	0.020	0.003	0.009	0.006
19C	0.037	0.079	0.058	0.047	0.153	0.100
20C	0.046	0.013	0.029	0.076	0.033	0.054
21C	0.040	0.008	0.024	0.071	0.043	0.057
22C	0.003	0.002	0.002	0.000	0.001	0.000
23C	−0.006	−0.014	−0.010	0.000	−0.001	−0.001
24C	−0.039	−0.020	−0.029	−0.029	−0.012	−0.020
25H	0.018	0.031	0.025	0.017	0.032	0.025
26H	0.022	0.038	0.030	0.014	0.030	0.022
27H	0.031	0.028	0.030	0.021	0.027	0.024
28H	−0.017	0.002	−0.008	0.002	0.008	0.005
29H	0.021	0.030	0.026	0.003	0.006	0.004
30H	0.009	0.028	0.019	0.003	0.009	0.006
31H	0.054	0.039	0.047	0.036	0.026	0.031
32H	0.019	0.041	0.030	0.002	0.006	0.004
33H	0.062	0.048	0.055	0.038	0.040	0.039
34H	0.064	0.049	0.057	0.044	0.032	0.038
35H	0.010	0.022	0.016	0.001	0.003	0.002
36H	0.013	0.030	0.021	0.002	0.005	0.003
37H	0.011	0.026	0.019	0.002	0.005	0.003
38H	0.015	0.028	0.021	0.001	0.002	0.002
39H	−0.003	0.005	0.001	0.001	0.002	0.001
40H	0.008	0.012	0.010	0.001	0.002	0.001
41H	0.039	0.014	0.026	0.037	0.012	0.025
42H	0.045	0.028	0.037	0.024	0.010	0.017
43H	0.038	0.014	0.026	0.037	0.012	0.025

Omeprazole is 17C > 19C > 39H > 14C > 4O > 31H > 11C > 21C > 1S > 33H > 3O > 6N > 25H > 26H > 20C > 29H > 5N > 7N > 15C > 30H > 10C > 37H > 38H > 35H > 36H > 2O > 13C > 22C > 9C > 12C > 16C > 18C > 28H > 8C > 23C > 27H > 24C. The order of reactivity changes significantly in the water phase, with carbon atoms at positions 17 (17C) and 19 (19C) being the most reactive sites, followed by hydrogen atoms at positions 39 (39H) and carbon atom at position 14 (14C). The oxygen atom at position 4 (4O), which was the most reactive site in the gas phase, has dropped to the fifth position in the water phase. Overall, the change in order of reactive sites in water can be attributed to the solvation effects, which influence the molecular geometry and electron density distribution. The solvent molecules interact with the inhibitor, leading to changes in the electronic properties of the molecule and altering the reactivity of certain sites. These findings can be useful for designing and optimising Omeprazole-based drugs for better efficacy and specificity.

Table 7 shows the order of reactive sites (Fukui indices) of the compound Tinidazole using different DFT/B3LYP/SVP methods in both gas and solvent (water). The table contains the results for each atom in the molecule, labelled as 1S to 29H. From the table, it can be observed that the Fukui indices for each atom differ based on the DFT/B3LYP/SVP method used and whether it was in the gas or water phase. The table shows that the order of reactive sites varies depending on the DFT method and the phase (gas or water) used. However, some general trends can be observed. In both gas and water phases, the most reactive site is the 13th carbon atom, followed by the 4th and 5th oxygen atoms. The least reactive sites are the 9th and 10th carbon atoms. The values of the Fukui indices also differ significantly between the gas and water phases, with the values generally being larger in the water phase. This difference can be attributed to the polar nature of water, which can affect the electronic structure of the molecule and alter the reactivity of the reactive sites. For example, atoms 2O, 3O and 4O have positive f^+ values, indicating that they are potential electrophilic attack sites. At the same time, atoms 1S and 8N have negative f^- values, indicating they are potential nucleophilic attack sites.

Table 8 shows the order of reactive sites (Fukui indices) of compound Tinidazole using different DFT/CAM-B3LYP/TZVP methods in both gas and solvent (water). The table includes the inhibitor, the DFT method, the solvent (gas or water), and the values of the Fukui indices for each reactive site of the molecule. In general, the values of the Fukui indices show that the most reactive sites in the molecule are the oxygen atoms (2O, 3O, 4O and 5O) and the carbon atom (13C) with the highest values of f^+ and f^-. The sulphur atom (1S) and nitrogen atoms (6N, 7N and 8N) also show significant reactivity, particularly in the gas phase. The effect of the solvent on the reactivity of the molecule is also apparent from the table. In general, the values of the Fukui indices are lower in water compared to the gas phase, indicating that the molecule is less reactive in the solvent. However, there are some exceptions to this trend, particularly for the carbon atoms (12C, 13C, 15C and 16C) and hydrogen atoms (17H, 18H, 19H, 20H, 26H, 27H, 28H and 29H), which show higher values of f^+ and f^- in water. Overall, Table 8 provides valuable information about the reactivity of different sites in the

Table 7. Order of reactive sites (Fukui indices) of compound Tinidazole by using different DFT/B3LYP/SVP methods in both gas and in solvent (water).

Inhibitor –TIN	B3LYP/SVP			B3LYP/SVP		
	Gas			*Water*		
	f^+	f^-	f^0	f^+	f^-	f^0
1S	−0.014	−0.003	−0.008	−0.008	−0.002	−0.005
2O	0.035	0.020	0.027	0.017	0.009	0.013
3O	0.021	−0.010	0.006	0.016	0.003	0.010
4O	0.099	0.189	0.144	0.101	0.211	0.156
5O	0.086	0.179	0.133	0.082	0.192	0.137
6N	0.014	0.016	0.015	0.009	0.012	0.010
7N	0.058	0.031	0.044	0.059	0.026	0.043
8N	−0.010	0.064	0.027	−0.003	0.084	0.041
9C	−0.011	−0.030	−0.020	−0.004	−0.013	−0.008
10C	−0.031	−0.031	−0.031	−0.022	−0.026	−0.024
11C	−0.005	−0.004	−0.004	0.000	0.000	0.000
12C	0.065	0.056	0.060	0.096	0.062	0.079
13C	0.111	0.000	0.055	0.152	0.020	0.086
14C	−0.006	−0.004	−0.005	−0.001	−0.001	−0.001
15C	0.090	0.108	0.099	0.131	0.139	0.135
16C	−0.008	−0.014	−0.011	0.002	−0.003	−0.001
17H	0.015	0.007	0.011	0.018	0.020	0.019
18H	0.046	0.048	0.047	0.025	0.022	0.023
19H	0.037	0.043	0.040	0.032	0.028	0.030
20H	0.044	0.031	0.038	0.039	0.035	0.037
21H	0.018	0.006	0.012	0.008	0.004	0.006
22H	0.029	0.021	0.025	0.010	0.005	0.007
23H	0.033	0.027	0.030	0.006	0.003	0.005
24H	0.017	0.015	0.016	0.005	0.003	0.004
25H	0.010	0.007	0.009	0.005	0.003	0.004
26H	0.083	0.081	0.082	0.078	0.073	0.076
27H	0.050	0.043	0.047	0.045	0.026	0.036
28H	0.065	0.055	0.060	0.058	0.035	0.046
29H	0.055	0.049	0.052	0.045	0.029	0.037

Table 8. Order of reactive sites (Fukui indices) of compound Tinidazole by using different DFT/ CAM-B3LYP/TZVP methods in both gas and in solvent (water).

Inhibitor –TIN	CAM-B3LYP/TZVP			CAM-B3LYP/TZVP		
	Gas			*Water*		
	f^+	f^-	f^0	f^+	f^-	f^0
1S	−0.013	−0.001	−0.007	−0.012	−0.001	−0.007
2O	0.022	0.022	0.022	0.012	0.009	0.011
3O	−0.009	−0.007	−0.008	0.008	0.005	0.007
4O	0.109	0.209	0.159	0.104	0.236	0.170
5O	0.100	0.201	0.150	0.084	0.216	0.150
6N	0.019	0.030	0.024	0.017	0.026	0.021
7N	0.069	0.017	0.043	0.081	0.024	0.052
8N	0.006	0.101	0.053	0.020	0.125	0.073
9C	−0.027	−0.046	−0.037	−0.004	−0.011	−0.007
10C	−0.018	−0.034	−0.026	−0.019	−0.045	−0.032
11C	0.008	0.007	0.007	0.005	0.002	0.004
12C	0.049	0.045	0.047	0.075	0.047	0.061
13C	0.142	−0.050	0.046	0.181	−0.020	0.080
14C	0.002	0.001	0.002	0.001	0.001	0.001
15C	0.090	0.140	0.115	0.126	0.166	0.146
16C	0.025	0.000	0.013	0.032	0.008	0.020
17H	0.012	0.002	0.007	0.016	0.019	0.018
18H	0.047	0.050	0.049	0.020	0.017	0.019
19H	0.028	0.038	0.033	0.024	0.020	0.022
20H	0.036	0.028	0.032	0.032	0.033	0.033
21H	0.006	−0.001	0.003	0.004	0.002	0.003
22H	0.019	0.018	0.018	0.005	0.003	0.004
23H	0.026	0.024	0.025	0.003	0.002	0.003
24H	0.011	0.012	0.012	0.003	0.002	0.002
25H	0.003	0.004	0.004	0.002	0.002	0.002
26H	0.078	0.070	0.074	0.060	0.050	0.055
27H	0.051	0.037	0.044	0.037	0.018	0.028
28H	0.062	0.047	0.055	0.048	0.025	0.036
29H	0.045	0.038	0.042	0.034	0.018	0.026

Tinidazole molecule and how this reactivity is affected by the solvent environment. These insights can be useful in predicting the behaviour of the molecule in different chemical reactions and in the design of new drugs based on Tinidazole.

Table 9 shows the order of reactive sites (Fukui indices) of Tinidazole compound using different DFT/ωB97XD/def2-TZVP methods in both gas and in solvent (water). The compounds are labelled from 1S to 29H. The values of the Fukui indices for each reactive site are given in columns corresponding to the gas and water phase calculations. The positive values of the Fukui indices indicate nucleophilic sites, while negative values indicate electrophilic sites. In general, the most reactive site in Tinidazole is site 4O, followed by site 5O and site 13C. These sites are nucleophilic and can attack electrophiles. The least reactive site is site 2O, which is electrophilic and can be attacked by nucleophiles. The effect of solvent is observed in some sites, such as site 4O, where the Fukui index is higher in water than in the gas phase. This indicates that the site is more nucleophilic in water than in the gas phase. On the other hand, some sites, such as site 13C, show a decrease in the Fukui index in water compared to the gas phase, indicating that the site is less nucleophilic in water.

Therefore, we observed that in addition to their significance in predicting the effectiveness of corrosion inhibitors, Fukui indices can also be used to determine the electrophilic and nucleophilic sites in these inhibitors. The Fukui indices can be used to determine these regions by calculating the electrophilic and nucleophilic reactivity indices (ω^+ and ω^-). These indices describe the change in electronic density upon addition or removal of an electron from the molecule, and are related to the HOMO and LUMO energies. A high value of the electrophilic reactivity index (ω^+) indicates that a particular region of the molecule is more likely to accept electrons, making it an electrophilic site. Conversely, a high value of the nucleophilic reactivity index (ω^-) indicates that a particular region of the molecule is more likely to donate electrons, making it a nucleophilic site. In the context of corrosion inhibitors, the electrophilic and nucleophilic sites of the inhibitor molecule can play an important role in the inhibition mechanism. For example, the nucleophilic sites on the inhibitor molecule may interact with metal ions or other reactive species in the corrosion process, while the electrophilic sites may interact with the metal surface to form a protective layer. Overall, the Fukui indices provide a useful tool for understanding the reactivity of corrosion inhibitors and designing new inhibitors with specific electrophilic and nucleophilic properties.

Table 9. Order of reactive sites (Fukui indices) of compound Tinidazole by using different DFT/ωB97XD/def2-TZVP methods in both gas and in solvent (water).

Inhibitor –*TIN*	ωB97XD/def2-TZVP			ωB97XD/def2-TZVP		
	Gas			*Water*		
	f^+	f^-	f^0	f^+	f^-	f^0
1S	−0.015	−0.008	0.749	−0.014	−0.005	−0.009
2O	0.022	0.022	−0.488	0.011	0.008	0.010
3O	−0.009	−0.005	−0.467	0.006	0.005	0.006
4O	0.101	0.208	−0.394	0.096	0.233	0.164
5O	0.096	0.201	−0.441	0.080	0.214	0.147
6N	0.039	0.031	−0.039	0.037	0.024	0.031
7N	0.084	0.020	−0.258	0.094	0.027	0.060
8N	−0.001	0.101	0.444	0.012	0.126	0.069
9C	−0.036	−0.044	−0.243	−0.009	−0.014	−0.012
10C	−0.023	−0.031	−0.211	−0.025	−0.042	−0.034
11C	0.003	0.004	−0.191	0.002	0.001	0.001
12C	0.059	0.051	0.231	0.087	0.056	0.072
13C	0.160	−0.033	0.131	0.198	−0.005	0.097
14C	−0.006	−0.006	−0.387	−0.001	−0.001	−0.001
15C	0.082	0.137	−0.092	0.116	0.164	0.140
16C	0.013	−0.006	−0.413	0.019	0.001	0.010
17H	0.012	0.002	0.183	0.016	0.022	0.019
18H	0.043	0.046	0.144	0.018	0.015	0.016
19H	0.032	0.038	0.181	0.027	0.020	0.023
20H	0.039	0.030	0.181	0.033	0.034	0.033
21H	0.007	−0.001	0.143	0.004	0.003	0.004
22H	0.020	0.018	0.137	0.005	0.004	0.004
23H	0.025	0.023	0.134	0.003	0.002	0.003
24H	0.011	0.012	0.147	0.003	0.002	0.002
25H	0.004	0.004	0.154	0.002	0.002	0.002
26H	0.078	0.068	0.174	0.058	0.047	0.053
27H	0.053	0.038	0.186	0.040	0.019	0.029
28H	0.061	0.044	0.145	0.047	0.023	0.035
29H	0.044	0.038	0.162	0.033	0.018	0.025

3.3. Monte Carlo simulation

Monte Carlo simulation is a computational technique used to model and simulate complex physical and chemical systems. In the context of corrosion inhibition, Monte Carlo simulations can be used to study the adsorption behaviours of inhibitors on metal surfaces [41–43]. In this study, the authors aim to investigate the protective performance of expired Helicure drugs towards the dissolution of mild steel in 1M HCl medium using both theoretical and experimental approaches. The authors have used Monte Carlo simulations to examine the adsorption of inhibitor molecules on the Fe (1 1 0) surface in the presence of water molecules, $4H_3O^+$ and $4Cl^-$ ions. The authors have focused on two inhibitors, namely TND and OMP, and have investigated their synergetic effect on the Fe (1 1 0) surface in the presence of $4H_3O^+$, $4Cl^-$ ions and 186 H_2O molecules. The results of the simulations have been presented in Figure 2, which shows the most stable low-energy adsorption of the studied inhibitors on the Fe (1 1 0) surface. The synergetic effect of TND and OMP has also been observed, indicating a better protective performance of the combination of these inhibitors on the mild steel surface. The adsorption energies of the inhibitors onto the surface of iron were calculated and analysed to identify the most stable adsorbed configuration of the studied molecules on the surface of the iron. The higher negative adsorption energy values indicated the most stable configuration of the inhibitors on the iron surface. It is well-known that Monte Carlo simulation provides mechanistic insights regarding to adsorption on metal surfaces of molecular systems. It is seen from Figure 2 that inhibitor molecules inhibitor molecules are positioned to interact strongly with the metal surface the heteroatoms in their structures. Figure 3 presents a schematic adsorption mechanism of interaction with the metal surface of TID and OMP molecules.

The use of expired drugs as inhibitors is a great idea to protect and valorise those compounds. Then, the prediction of their efficiency theoretically is a smart and economical tool to evaluate their inhibition performance. Therefore, the adsorption energy values can facilitate the ranking of inhibitor products. Table 10 provides the adsorption energies for the

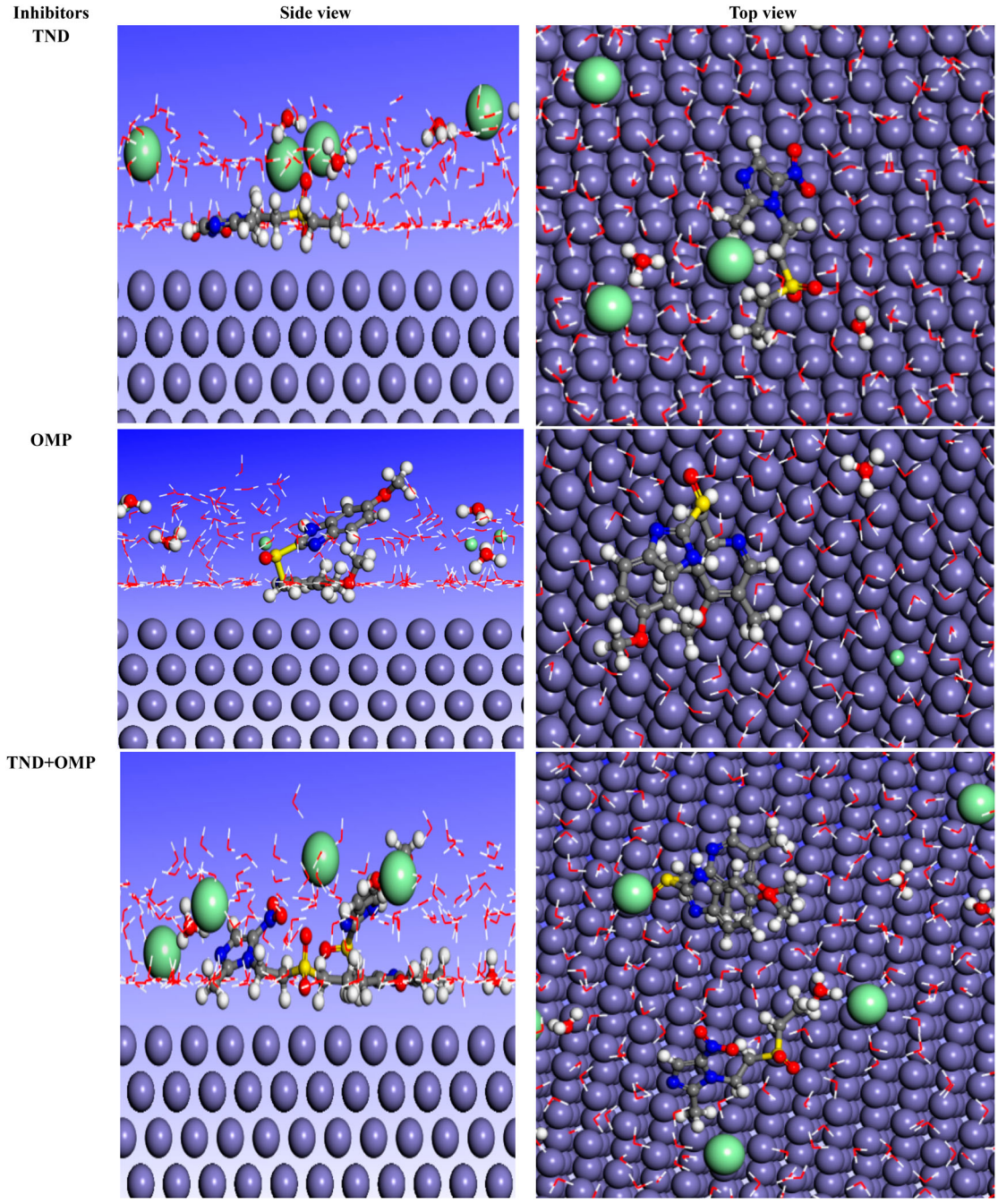

Figure 2. (Colour online) The most stable low energy configuration for the adsorption of studied products on Fe (1 1 0) surface obtained using the Monte Carlo simulation.

studied inhibitors, TND and OMP, on Fe (1 1 0) surface obtained using Monte Carlo simulation. The units used for the adsorption energies are kcal/mol. The table contains three systems: Fe (1 1 0)/TND, Fe (1 1 0)/OMP and Fe (1 1 0)/OMP. Adsorption energy is an important parameter in determining the effectiveness of a corrosion inhibitor. The adsorption energy is defined as the amount of energy released when a molecule is adsorbed on a surface. In the case of corrosion inhibition, the adsorption energy indicates how strongly the inhibitor molecule interacts with the metal surface, forming a protective layer that inhibits the corrosion process. The value obtained for the system TND on Fe (1 1 0) surface is −7162.29 kcal/mol. The value obtained for the system OMP on Fe (1 1 0) surface is −3431.69 kcal/mol. The value obtained for the system TND + OMP on Fe (1 1 0) surface is −7194.89 kcal/mol. From the results in Table 2, it can be observed that the adsorption energies for TND and OMP are quite different. TND has a significantly higher adsorption energy of −7162.29 kcal/mol compared to OMP, which has adsorption energy of −3431.69 kcal/mol. This indicates that TND is a more effective inhibitor than OMP, as it forms a stronger protective layer on the metal surface. Furthermore, the adsorption energy of TND + OMP on the Fe (1 1 0) surface is higher (−7194.89 kcal/mol) compared to the adsorption

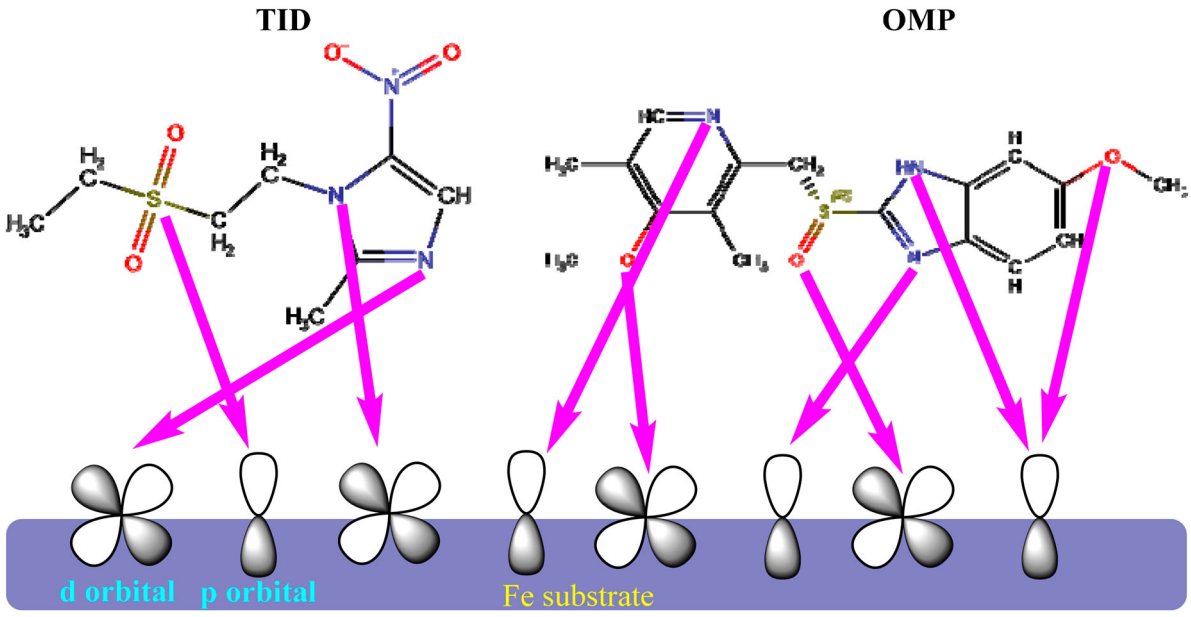

Figure 3. (Colour online) A schematic adsorption mechanism of interaction with the metal surface of TID and OMP molecules.

energy of OMP and TND alone. This suggests that the synergistic effect enhances the adsorption of TND + OMP on the metal surface, leading to better corrosion inhibition. Additionally, for the Fe (1 1 0)/TND system, the adsorption energy is −32.78 kcal/mol. This indicates that the TND inhibitor molecule strongly interacts with the Fe (1 1 0) surface in the presence of water molecules. Similarly, for the Fe (110)/OMP system, the adsorption energy is −6.91 kcal/mol, which indicates a moderate interaction between the OMP inhibitor and the iron surface. Interestingly, for the Fe (1 1 0)/TND + OMP system, the adsorption energy is −31.68 kcal/mol, which is higher than that of the Fe (1 1 0)/TND system. This implies that the TND + OMP molecule interacts more strongly with the iron surface in the absence of water molecules. This observation suggests that the presence of water molecules may affect the orientation and interaction strength of the inhibitor molecules with the iron surface [10]. From this result, we can predict that the inhibition efficiency values are increased in the sequence: TND + OMP > TND > OMP > the synergetic effect of TND and OMP compounds decrease the corrosion rate more than TND and OMP only resulted in a large coverage filled by the two inhibitors. In all studied systems, the adsorption energies of the inhibitor molecules are higher than that of H_2O molecules. This explains the possibility of the gradual substitution of water molecules from the surface of iron as a result of the formation of a stable and strong layer that can protect the iron from corrosion in an acid medium. These findings are important in understanding the mechanism of corrosion inhibition and can be used in the design of more effective inhibitors for the protection of metal surfaces.

Table 10. Adsorption energies for the studied inhibitor on Fe (1 1 0) surface obtained using the Monte Carlo simulation (all units in kcal/mol).

Systems	Adsorption energy Inhibitor	Adsorption energy Water
Fe(1 1 0)/TND	−7162.29	−32.78
Fe(1 1 0)/OMP	−3431.69	−06.91
Fe(1 1 0)/TND + OMP	−7194.89	−31.68

3.3.1. Electronic structure rules

Chemical hardness [44,45] concept represents the represents the resistance against the polarisation. It is well-known that there is an inverse correlation between hardness and polarisability parameters. The electronic structure rule reflecting the link between hardness and chemical stability is Maximum Hardness Principle [46–48]. This electronic structure rule proposed by Pearson in 1990s states that the stable chemical systems at equilibrium state tend to reach to maximum value of the chemical hardness. Namely the chemical hardness is a measure of the stability. For that reason, hard molecules cannot exhibit good corrosion inhibition performance. The obtained corrosion inhibition ranking via the computed chemical hardness values is TND > OMP. This order is compatible with both experimental data and the data derived from Monte Carlo Simulation calculations. Chattaraj's Minimum Polarisability Principle [49] states the minimisation of the polarisability in the stable states. This rule has been introduced in the light of the inverse correlation between hardness and polarisability. Minimum Polarisability Principle predict that OMP is more effective inhibitor than that of TND but this prediction is not in good agreement with the experimental study performed. Another electronic structure rule used in the chemical reactivity analysis of the compounds is Minimum Electrophilicity Principle [50,51]. According to Minimum Electrophilicity Principle, 'in exothermic reactions, the sum of the electrophilicity indexes of the products should be

Table 11. In silico values of Log (IGC50) and Log P by online chemical data website.

Inhibitors	Log (IGC50) in Log(mmol/L)	Log *P* in Log(mol/L)
TND	−0.14	−2.3
OMP	−0.54	−3.4

smaller than that of the reactant.' From this information, it can be said that Minimum Electrophilicity Principle implies the minimisation of the electrophilicity index in stable state and conformations. Both first and second electrophilicity indexes calculated for OMP is smaller than that of TND. Namely, Minimum Electrophilicity Principle states that OMP is more stable than TND. Because reactive molecules are good corrosion inhibitors, the corrosion inhibition efficiency ranking obtained through Minimum Electrophilicity Principle is TND > OMP. This order supports the experimental data and calculated adsorption energies. In general, corrosion scientists don't consider Minimum Electrophilicity Principle in the theoretical part of their studies. Here, we report that electronic structure principles or rules should be used in such corrosion studies.

3.4. Toxicity and solubility assessment

In the field of corrosion inhibition, it is essential to investigate the toxicity and solubility of the inhibitors used. Toxicity is measured in terms of the concentration required to provide a 50% inhibitory growth of species (usually in water), which is represented by the Log (IGC50) value. On the other hand, the Log *P* value is a measure of lipophilicity, which is calculated as the logarithm of the octanol–water partition coefficient. A positive Log *P* value indicates lipophilicity, while a negative value indicates higher solubility in water. The results of toxicity and solubility tests are often presented in tables. Table 11, for instance, regroups the toxicity and solubility results of a study conducted by Y. Samar et al. on the inhibitive effect of expired helicure drugs on mild steel corrosion in hydrochloric acid solution. The experiment was conducted at a concentration range between 50 and 300 ppm. The Log *P* values obtained from the study are negative, indicating that the Helicure drugs have good solubility in acidic media. This means that they are likely to dissolve well in hydrochloric acid solution, which is an important factor to consider in corrosion inhibition studies. The IGC50 values obtained from the study are less than the concentration used in the experimental part, indicating that these inhibitors are environmentally friendly products at the studied concentration range. This is because they do not have a toxic effect on the aquatic species used in toxicity tests, such as *Tetrahymena pyriformis* or *Daphnia magna*.

4. Conclusion

In conclusion, the study provides a detailed investigation into the adsorption behaviour and inhibition mechanism of Omeprazole and Tinidazole on metallic surfaces in aqueous acidic conditions. The use of quantum chemical calculations and MC simulations allowed for a thorough understanding of the inhibitors' properties and interactions with the steel surface. Fukui indices analysis provided insight into the inhibitors' reactive sites, while Monte Carlo simulations determined the optimal adsorption configuration of the inhibitors onto the steel surface. The results showed that TND is a more effective inhibitor than OMP, as it forms a stronger protective layer on the metal surface. The synergistic effect of TND + OMP was also found to enhance the adsorption on the metal surface, leading to better corrosion inhibition. The interaction strength between the inhibitors and the Fe (1 1 0) surface was found to be affected by the presence of water molecules. The study provides important insights into the mechanism of corrosion inhibition and can be used in the design of more effective inhibitors for the protection of metal surfaces in acid mediums. The IGC50 values obtained from the study showed that the inhibitors are environmentally friendly products at the concentration range tested, since they did not have a toxic effect on the aquatic species used in the toxicity tests. These findings are valuable in determining the suitability of OMP and TND (helicure drugs) as corrosion inhibitors and highlight the importance of considering the toxicity and solubility of inhibitors in corrosion inhibition studies [52,53].

Disclosure statement

No potential conflict of interest was reported by the author(s).

Acknowledgements

The authors extend their appreciation to the Deanship of Scientific Research at King Khalid University, Saudi Arabia for funding this work through Large Research Groups Programme under grant number L.R.G.P2/3/44.

ORCID

Hassane Lgaz http://orcid.org/0000-0001-8506-5759

References

[1] Mandal S, Zamindar S, Sarkar S, et al. Quantum chemical and molecular dynamics simulation approach to investigate adsorption behaviour of organic azo dyes on TiO2 and ZnO surfaces. J Adhes Sci Technol. 2023;37(10):1649–1665. doi:10.1080/01694243.2022.2086199

[2] Wang P, Xiong L, He Z, et al. Extraordinary corrosion inhibition efficiency of omeprazole in 1 M HCl solution: experimental and theoretical investigation. Surf Interface Anal. 2023;55(4):226–242. doi:10.1002/sia.7181

[3] Guo L, Huang Y, Wu Y, et al. Experimental and theoretical studies of the corrosion inhibition performance of a quaternary phosphonium-based ionic liquid for mild steel in HCl medium. Sustainability. 2023;15(4):3103. doi:10.3390/su15043103

[4] Sengupta S, Murmu M, Mandal S, et al. Competitive corrosion inhibition performance of alkyl/acyl substituted 2-(2-hydroxybenzylideneamino) phenol protecting mild steel used in adverse acidic medium: A dual approach analysis using FMOs/molecular dynamics simulation corroborated experimental findings. Colloids Surf A Physicochem Eng Asp. 2021;617:126314. doi:10.1016/j.colsurfa.2021.126314

[5] Mandal S, Murmu M, Sengupta S, et al. Effect of molecular chain length on the tribological properties of two diazomethine functionalised molecules as efficient surface protective lubricant additive: experimental and in silico investigation. J Adhes Sci Technol. 2023;37(2):213–239. doi:10.1080/01694243.2022.2026706

[6] Kaya S, Guo L, Kaya C, et al. Quantum chemical and molecular dynamic simulation studies for the prediction of inhibition efficiencies of some piperidine derivatives on the corrosion of iron. J Taiwan Inst Chem Eng. 2016;65:522–529. doi:10.1016/j.jtice.2016.05.034

[7] Madkour LH, Kaya S, Obot IB. Computational, Monte Carlo simulation and experimental studies of some arylazotriazoles (AATR)

and their copper complexes in corrosion inhibition process. J Mol Liq. 2018;260:351–374. doi:10.1016/j.molliq.2018.01.055
[8] Mobin M, Aslam R, Salim R, et al. An investigation on the synthesis, characterization and anti-corrosion properties of choline based ionic liquids as novel and environmentally friendly inhibitors for mild steel corrosion in 5% HCl. J Colloid Interface Sci. 2022;620:293–312. doi:10.1016/j.jcis.2022.04.036
[9] Kaya S, Tüzün B, Kaya C, et al. Determination of corrosion inhibition effects of amino acids: quantum chemical and molecular dynamic simulation study. J Taiwan Inst Chem Eng. 2016;58:528–535. doi:10.1016/j.jtice.2015.06.009
[10] Obot IB, Kaya S, Kaya C, et al. Density functional theory (DFT) modeling and Monte Carlo simulation assessment of inhibition performance of some carbohydrazide Schiff bases for steel corrosion. Phys E Low-Dimens Syst Nanostructures. 2016;80:82–90. doi:10.1016/j.physe.2016.01.024
[11] Afia L, Hamed O, Larouj M, et al. Novel natural based diazepines as effective corrosion inhibitors for carbon steel in HCl solution: experimental, theoretical and Monte Carlo simulations. Trans Indian Inst Metals. 2017;70:2319–2333. doi:10.1007/s12666-017-1094-x
[12] Özbakır Işın D, Karakuş N, Lgaz H, et al. Theoretical insights about inhibition efficiencies of some 8-hydroxyqionoline derivatives against the corrosion of mild steel. Mol Simul. 2020;46(17):1398–1404. doi:10.1080/08927022.2020.1834102
[13] Guo L, Tan J, Kaya S, et al. Multidimensional insights into the corrosion inhibition of 3, 3-dithiodipropionic acid on Q235 steel in H2SO4 medium: a combined experimental and in silico investigation. J Colloid Interface Sci. 2020;570:116–124. doi:10.1016/j.jcis.2020.03.001
[14] Anadebe VC, Nnaji PC, Onukwuli OD, et al. Multidimensional insight into the corrosion inhibition of salbutamol drug molecule on mild steel in oilfield acidizing fluid: experimental and computer aided modeling approach. J Mol Liq. 2022;349:118482. doi:10.1016/j.molliq.2022.118482
[15] Al-Nami SY. Investigation of adsorption and inhibitive effect of expired helicure drug on mild steel corrosion in hydrochloric acid solution. Int J Electrochem Sci. 2020;15:2685–2699. doi:10.20964/2020.03.34
[16] Cohen AJ, Mori-Sánchez P, Yang W. Challenges for density functional theory. Chem Rev. 2012;112(1):289–320. doi:10.1021/cr200107z
[17] Grimme S, Antony J, Ehrlich S, et al. A consistent and accurate ab initio parametrization of density functional dispersion correction (DFT-D) for the 94 elements H-Pu. J Chem Phys. 2010/04/21 2010;132(15):154104. doi:10.1063/1.3382344
[18] Schäfer A, Horn H, Ahlrichs R. Fully optimized contracted Gaussian basis sets for atoms Li to Kr. J Chem Phys. 1992;97(4):2571–2577. doi:10.1063/1.463096
[19] Schäfer A, Huber C, Ahlrichs R. Fully optimized contracted Gaussian basis sets of triple zeta valence quality for atoms Li to Kr. J Chem Phys. 1994;100(8):5829–5835. doi:10.1063/1.467146
[20] Weigend F, Ahlrichs R. Balanced basis sets of split valence, triple zeta valence and quadruple zeta valence quality for H to Rn: design and assessment of accuracy. Phys Chem Chem Phys. 2005;7(18):3297–3305. doi:10.1039/b508541a
[21] Becke AD. Density-functional thermochemistry. III. The role of exact exchange. J Chem Phys. 1993;98(7):5648–5652. doi:10.1063/1.464913
[22] Yanai T, Tew DP, Handy NC. A new hybrid exchange–correlation functional using the Coulomb-attenuating method (CAM-B3LYP). Chem Phys Lett. 2004;393(1-3):51–57. doi:10.1016/j.cplett.2004.06.011
[23] Chai J-D, Head-Gordon M. Long-range corrected hybrid density functionals with damped atom–atom dispersion corrections. Phys Chem Chem Phys. 2008;10(44):6615–6620. doi:10.1039/b810189b
[24] Tomasi J, Mennucci B, Cammi R. Quantum mechanical continuum solvation models. Chem Rev. 2005;105(8):2999–3094. doi:10.1021/cr9904009
[25] Frisch MJ, et al. Gaussian 09, revision A.02, Gaussian. Wallingford (CT): Inc.; 2016.
[26] Islam N, Kaya S, editors. Conceptual density functional theory and its application in the chemical domain. New York: CRC Press; 2018.
[27] Parr RG, Szentpály LV, Liu S. Electrophilicity index. J Am Chem Soc. 1999;121(9):1922–1924. doi:10.1021/ja983494x
[28] von Szentpály L. Physical basis and limitations of equalization rules and principles: valence-state electronegativity and valence-pair-affinity versus operational chemical potential. Quantum Matter. 2015;4(1):47–55. doi:10.1166/qm.2015.1170
[29] Erdoğan Ş, Safi ZS, Kaya S, et al. A computational study on corrosion inhibition performances of novel quinoline derivatives against the corrosion of iron. J Mol Struct. 2017;1134:751–761. doi:10.1016/j.molstruc.2017.01.037
[30] Kaya S, Banerjee P, Saha SK, et al. Theoretical evaluation of some benzotriazole and phospono derivatives as aluminum corrosion inhibitors: DFT and molecular dynamics simulation approaches. RSC Adv. 2016;6(78):74550–74559. doi:10.1039/C6RA14548E
[31] Yan Y, Wang X, Zhang Y, et al. Theoretical evaluation of inhibition performance of purine corrosion inhibitors. Mol Simul. 2013;39(13):1034–1041. doi:10.1080/08927022.2013.792928
[32] Gómez B, Likhanova NV, Dominguez Aguilar MA, et al. Theoretical study of a new group of corrosion inhibitors. J Phys Chem A. 2005;109(39):8950–8957. doi:10.1021/jp052188k
[33] Khaled KF. Monte Carlo simulations of corrosion inhibition of mild steel in 0.5 M sulphuric acid by some green corrosion inhibitors. J Solid State Electrochem. 2009;13:1743–1756. doi:10.1007/s10008-009-0845-y
[34] Verma C, Lgaz H, Verma DK, et al. Molecular dynamics and Monte Carlo simulations as powerful tools for study of interfacial adsorption behavior of corrosion inhibitors in aqueous phase: a review. J Mol Liq. 2018;260:99–120. doi:10.1016/j.molliq.2018.03.045
[35] Costa SN, Almeida-Neto FW, Campos OS, et al. Carbon steel corrosion inhibition in acid medium by imidazole-based molecules: experimental and molecular modelling approaches. J Mol Liq. 2021;326:115330. doi:10.1016/j.molliq.2021.115330
[36] Saha SK, Banerjee P. A theoretical approach to understand the inhibition mechanism of steel corrosion with two aminobenzonitrile inhibitors. RSC Adv. 2015;5(87):71120–71130. doi:10.1039/C5RA15173B
[37] Obot IB, Gasem ZM. Theoretical evaluation of corrosion inhibition performance of some pyrazine derivatives. Corros Sci. 2014;83:359–366. doi:10.1016/j.corsci.2014.03.008
[38] Khaled KF. Modeling corrosion inhibition of iron in acid medium by genetic function approximation method: A QSAR model. Corros Sci. 2011;53(11):3457–3465. doi:10.1016/j.corsci.2011.01.035
[39] Guo L, Safi ZS, Kaya S, et al. Anticorrosive effects of some thiophene derivatives against the corrosion of iron: a computational study. Front Chem. 2018;6:155. doi:10.3389/fchem.2018.00155
[40] Rodríguez-Valdez LM, Martínez-Villafañe A, Glossman-Mitnik D. Computational simulation of the molecular structure and properties of heterocyclic organic compounds with possible corrosion inhibition properties. Jo Mol Struct: Theochem. 2005;713(1-3):65–70. doi:10.1016/j.theochem.2004.10.036
[41] Verma C, Lgaz H, Verma DK, et al. Molecular dynamics and Monte Carlo simulations as powerful tools for study of interfacial adsorption behavior of corrosion inhibitors in aqueous phase: a review. J Mol Liq. 2018;260:99–120. doi:10.1016/j.molliq.2018.03.045
[42] Khaled KF. Monte Carlo simulations of corrosion inhibition of mild steel in 0.5 M sulphuric acid by some green corrosion inhibitors. J Solid State Electrochem. 2009;13:1743–1756. doi:10.1007/s10008-009-0845-y
[43] Shaw P, Obot IB, Yadav M. Functionalized 2-hydrazinobenzothiazole with carbohydrates as a corrosion inhibitor: electrochemical, XPS, DFT and Monte Carlo simulation studies. Mater Chem Front. 2019;3(5):931–940. doi:10.1039/C9QM00096H
[44] Kaya S, Kaya C. A new equation for calculation of chemical hardness of groups and molecules. Mol Phys. 2015;113(11):1311–1319. doi:10.1080/00268976.2014.991771
[45] Kaya S, Kaya C. A new method for calculation of molecular hardness: a theoretical study. Comput Theor Chem. 2015;1060:66–70. doi:10.1016/j.comptc.2015.03.004

[46] Pearson RG. The principle of maximum hardness. Acc Chem Res. 1993;26(5):250–255. doi:10.1021/ar00029a004
[47] Kaya S, Kaya C. A simple method for the calculation of lattice energies of inorganic ionic crystals based on the chemical hardness. Inorg Chem. 2015;54(17):8207–8213. doi:10.1021/acs.inorgchem.5b00383
[48] Kaya S, Robles-Navarro A, Mejía E, et al. On the prediction of lattice energy with the Fukui potential: some supports on hardness maximization in inorganic solids. J Phys Chem A. 2022;126(27):4507–4516. doi:10.1021/acs.jpca.1c09898
[49] Chattaraj PK, Sengupta S. Popular electronic structure principles in a dynamical context. J Phys Chem. 1996;100(40):16126–16130. doi:10.1021/jp961096f
[50] von Szentpály L, Kaya S, Karakuş N. Why and when is electrophilicity minimized? New theorems and guiding rules. J Phys Chem A. 2020;124(51):10897–10908. doi:10.1021/acs.jpca.0c08196
[51] Chattaraj PK, Giri S. A minimum electrophilicity perspective of the HSAB principle. Ind J Phys. 2007;81:871–879.
[52] de Lima-Neto P, de Araujo AP, Araujo WS, et al. Study of the anticorrosive behaviour of epoxy binders containing non-toxic inorganic corrosion inhibitor pigments. Prog Org Coat. 2008;62(3):344–350. doi:10.1016/j.porgcoat.2008.01.012
[53] Huang L, Wang SS, Li HJ, et al. Highly effective Q235 steel corrosion inhibition in 1 M HCl solution by novel green strictosamide from uncaria laevigata: experimental and theoretical approaches. J Environ Chem Eng. 2022;10(3):107581. doi:10.1016/j.jece.2022.107581